

Role of Hydrogen in the spin-orbital-entangled quantum liquid candidate $\text{H}_3\text{LiIr}_2\text{O}_6$

Ying Li,^{1,*} Stephen M. Winter,¹ and Roser Valentí¹

¹*Institut für Theoretische Physik, Goethe-Universität Frankfurt,
Max-von-Laue-Strasse 1, 60438 Frankfurt am Main, Germany*

(Dated: November 14, 2018)

Motivated by recent reports of $\text{H}_3\text{LiIr}_2\text{O}_6$ as a spin-orbital-entangled quantum liquid, we investigate via a combination of density functional theory and non-perturbative exact diagonalization the microscopic nature of its magnetic interactions. We find that while the interlayer O-H-O bond geometry strongly affects the local magnetic couplings, these bonds are likely to remain symmetrical due to large zero-point fluctuations of the H positions. In this case, the estimated magnetic model lies close to the classical tricritical point between ferromagnetic, zigzag and incommensurate spiral orders, what may contribute to the lack of magnetic ordering. However, we also find that substitution of H by D (deuterium) as well as disorder-induced inhomogeneities destabilize the O-H/D-O bonds modifying strongly the local magnetic couplings. These results suggest that the magnetic response in $\text{H}_3\text{LiIr}_2\text{O}_6$ is likely sensitive to both the stoichiometry and microstructure of the samples and emphasize the importance of a careful treatment of hydrogen for similar systems.

Since the proposal by A. Kitaev of a Z_2 spin liquid groundstate in a honeycomb lattice with bond-dependent Ising-like nearest neighbor interactions [1], intensive effort has been devoted to find material realizations of such a state [2–5]. Promising candidates are the layered honeycomb iridates Na_2IrO_3 [6] and $\alpha\text{-Li}_2\text{IrO}_3$ [7, 8] as well RuCl_3 [9–13]. and the three-dimensional lattices $\beta\text{-Li}_2\text{IrO}_3$ and $\gamma\text{-Li}_2\text{IrO}_3$ [14–18]. However, these materials order magnetically either in a zig-zag structure as in Na_2IrO_3 and RuCl_3 or in incommensurate spiral structures as in the Li_2IrO_3 polymorphs [19]. This magnetic long-range order has been attributed to the presence of further non-Kitaev interactions [20–24] partly reminiscent of underlying delocalized quasimolecular orbitals [25–27]. Attempts to modulate the magnetic interactions in terms of pressure resulted in dimerized structures in the layered cases with no sign of spin liquid behavior [28–30].

Recently, however, a new member of this family was synthesized by substituting in $\alpha\text{-Li}_2\text{IrO}_3$ interlayer lithium ions by protons ($^1\text{H}^+$) [31–34]. Measurements of magnetic susceptibility, specific heat, and nuclear magnetic resonance (NMR) on the resulting $\text{H}_3\text{LiIr}_2\text{O}_6$ showed no sign of magnetic order down to 0.05 K [33]. Initial studies of the deuterium variant suggest a similar response [34]. However, the low temperature heat capacity of $\text{H}_3\text{LiIr}_2\text{O}_6$ only accounts for a small $\sim 1 - 2\%$ of the total $\ln(2)$ spin entropy, suggesting that the majority of spin excitations are gapped out [33]. This can be contrasted with the pure Kitaev model, for which thermally excited static fluxes produce a pronounced low temperature peak accounting for 50% of $\ln(2)$ entropy [35]. These deviations from the Kitaev model have been interpreted in terms of a model with sizeable interlayer couplings mediated by the H atoms [36]. Alternatively, it has been suggested that the low temperature scaling of the specific heat, susceptibility, and NMR response may be explained by a small fraction of defect-induced local moments [37].

Attempts to estimate the magnetic interactions via *ab initio* studies are currently lacking.

In this work, we investigate the specific influence of hydrogen $^1\text{H}^+$ and deuterium ($\text{D}^+ = ^2\text{H}^+$) substitution on the local magnetic interactions of $(\text{H}/\text{D})_3\text{LiIr}_2\text{O}_6$ for both pristine and structurally disordered samples. For that we perform extensive density functional theory simulations combined with numerical model calculations. For edge-sharing iridates, the magnetic interactions are known to be highly sensitive to local structural details such as the Ir-O-Ir bond angles [2, 20–22, 38, 39]. Here, we show that the H-bond geometry similarly strongly affects the magnetic Hamiltonian. This emphasizes the importance of determining the precise H/D positions, which are usually unavailable from x-ray analysis. We therefore analyze the stability of the symmetrical O-H-O bonds with respect to (i) zero-point fluctuations of the H positions, (ii) deuteration and (iii) the presence of structural disorder. We find that such bonds are likely to be unstable to both latter perturbations (ii)-(iii), leading to strongly modified interactions in deuterated or disordered samples.

We first study the influence of the H-bond geometry on the electronic structure and magnetic interactions. Starting from the ideal structure [32], the H coordinates were relaxed with the Vienna *ab initio* simulation package (VASP) [40, 41] in the GGA approximation constraining the symmetry to be: (a) $C2/m$, (b) $C2c2/m$, (c) $P2_1/m$, and (d) Cm (see Fig. 1). For the ideal $C2/m$ structure (Fig. 1 (a)), the symmetrical interlayer O-H-O bonds are maintained with minimal modification; the relaxed O(1)-H and O(2)-H distances are $d_{\text{O}(1)\text{H}} = 1.23 \text{ \AA}$ and $d_{\text{O}(2)\text{H}} = 1.27 \text{ \AA}$, respectively. In contrast, the lower symmetry structures (Fig. 1 (b)-(d)) feature various hypothetical patterns of asymmetric long/short O · · · H-O bonds. In each case, the short O-H distances are in the range $d_{\text{OH}} = 1.05 - 1.10 \text{ \AA}$, while the longer O · · · H distances are $d_{\text{OH}} = 1.36 - 1.50 \text{ \AA}$. The hopping

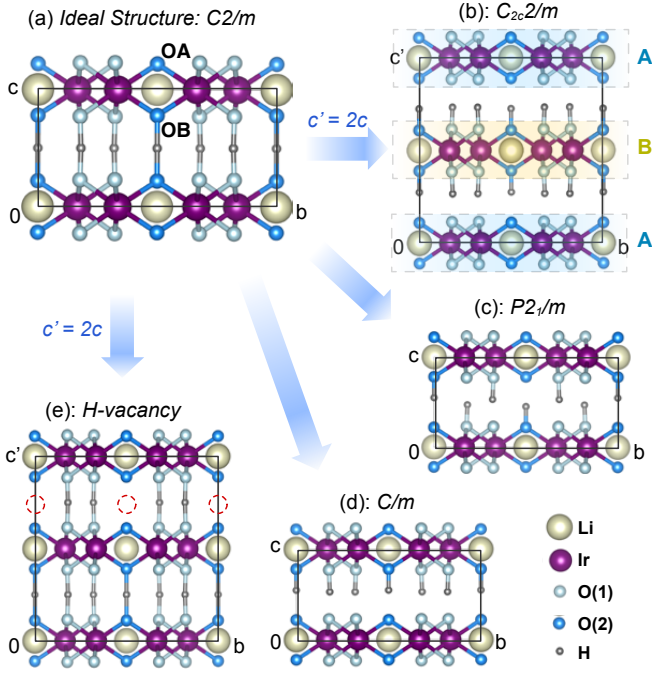


FIG. 1. Hypothetical structures considered to investigate the dependence of magnetic interactions on H-bond geometry. The two bridging ligand oxygen contributed to Ir-Ir hoppings along the Z-bonds are labeled as OA and OB. For structure (b) and (e), doubling of the c -axis leads to two inequivalent layers A and B.

parameters of the relaxed structures were obtained by full-potential linearized augmented plane-wave (LAPW) calculations [42] within GGA. The magnetic interactions were estimated by 2-site exact diagonalization of the corresponding tight-binding model with Hubbard, Hund's and spin-orbit coupling interactions [22, 43], and are presented in Table I. Full computational and structure details can be found in the Supplemental Material [44].

At the level of a single Ir, the d -orbital Wannier functions extend to the neighboring O atoms. Modification of the oxygen bonding environment via H doping (delithiation in this case) therefore affects both the effective Ir crystal field splitting, and the d - d hopping integrals. In the parent α - Li_2IrO_3 material, the Li^+ and Ir^{4+} ions form a pseudo-octahedral environment around each O atom (Fig. 2 (b)). In $\text{H}_3\text{LiIr}_2\text{O}_6$, the O environment becomes pseudo-tetrahedral, with the O-(H/D) bond vectors lying along the cubic [111] direction (Fig. 2(c)). Hybridization of the O $2p$ and H $1s$ orbitals produces an effective trigonal crystal field at the oxygen sites. The resultant mixing of the O p -orbitals modifies the Ir d -orbital Wannier functions in two key ways. First, the effective off-diagonal crystal field terms are enhanced with increasing O-H hybridization. Second, oxygen mediated d - d hopping integrals involving single (multiple) O p -orbitals are suppressed (enhanced). For example, within $C2/m$ symme-

try, the d - d hopping integrals for the Z-bond can be written in terms of $t_1 = t_{xz,xz} = t_{yz,yz}$, $t_2 = t_{xz,yz} = t_{yz,xz}$, $t_3 = t_{xy,xy}$, and $t_4 = t_{xz,xy} = t_{yz,xy} = t_{xy,xz} = t_{xy,yz}$ (Fig. 2 (a)). Comparing the results for the various structures, we find that $|t_2|$ is systematically reduced with decreasing O-H distance, due to suppression of the hopping paths like $\text{Ir}(d_{xz}) \rightarrow \text{O}(p_z) \rightarrow \text{Ir}(d_{yz})$. Similarly, $|t_3|$ and $|t_4|$ are enhanced through new hopping paths such as $\text{Ir}(d_{xz}) \rightarrow \text{O}(p_z) \rightarrow \text{H}(s) \rightarrow \text{O}(p_x) \rightarrow \text{Ir}(d_{xy})$. The hopping integrals for various structures are in the Supplemental Material [44].

The modification of the hopping integrals affects the magnetic couplings, which can be written as $H_{\text{spin}} = \sum_{\langle ij \rangle} \mathbf{S}_i \cdot \mathbf{J}_{ij} \cdot \mathbf{S}_j$, where \mathbf{J}_{ij} is a 3×3 matrix and $\langle ij \rangle$ denotes a sum over all nearest neighbor sites. Here H_{spin} is a spin model of interacting spin-orbit entangled pseudospins, rather than real spins. Within $C2/m$ symmetry, the interactions along the nearest-neighbor Z-bond (Fig. 1(a)) are described by a symmetric matrix:

$$\mathbf{J}_s = \begin{pmatrix} J_1 & \Gamma_1 & \Gamma'_1 \\ \Gamma_1 & J_1 & \Gamma'_1 \\ \Gamma'_1 & \Gamma'_1 & J_1 + K_1 \end{pmatrix}, \quad (1)$$

For the ideal structure (Fig. 1 (a)), we estimate $J_1 = -1.3$, $K_1 = -15.4$, $\Gamma_1 = +1.5$, and $\Gamma'_1 = -5.1$ meV for the Z-bond where positive (negative) signs correspond to antiferromagnetic (ferromagnetic) interactions. For the lower symmetry X and Y bonds, additional constants are required to specify the interactions [22]. Averaging over these values yields $J_1 \approx -0.8$, $K_1 \approx -18.9$, $\Gamma_1 \approx +0.3$,

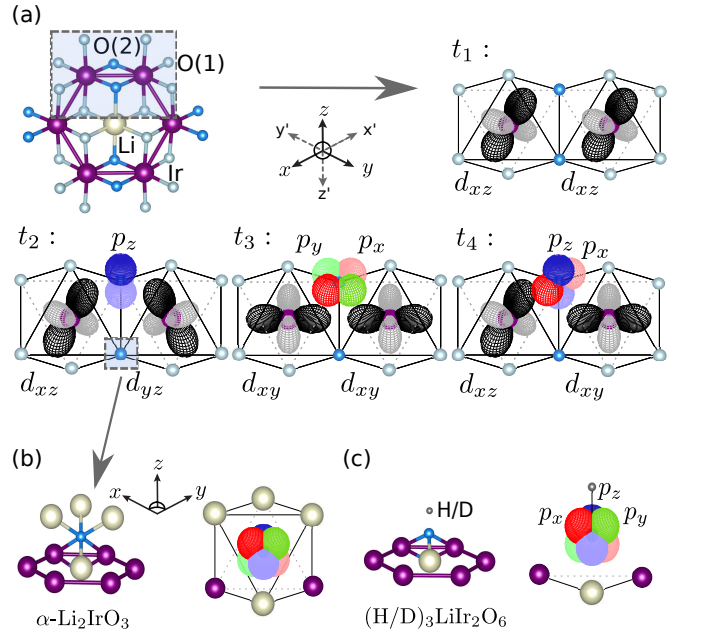


FIG. 2. (a) O p -orbital contributions to the effective Ir-Ir hopping integrals t_1 - t_4 for the Z-bond. (b)-(c): Comparison of the oxygen coordination environments in α - Li_2IrO_3 and $(\text{H/D})_3\text{LiIr}_2\text{O}_6$, respectively.

and $\Gamma'_1 \approx -5.4$ meV. Compared to α -Li₂IrO₃, the increased Ir-O-Ir bond angle of H₃LiIr₂O₆ suppresses t_3 and leads to the reduced Γ_1 . The large Γ'_1 values for the ideal structure of H₃LiIr₂O₆ are due to the enhanced crystal-field splitting. Note that the computed interactions $(J, K, \Gamma, \Gamma') = (-1.3, -15.4, +1.5, -5.1)$ meV are given in the reference frame xyz shown in Fig. 2. By performing a π -rotation around the cubic (111) direction, as outlined in Ref. 45, the xyz reference frame transforms to $x'y'z'$ (Fig. 2) and the above set of interactions transform to $(J, K, \Gamma, \Gamma') = (-11.1, +13.9, -8.3, -0.2)$ meV. This model lies close to the classical tricritical point [21] between ferromagnetic, zigzag, and incommensurate spiral orders, which may strongly contribute to the observed lack of magnetic order. The interlayer interactions are anisotropic, but have a magnitude $\lesssim 1.5$ meV, which is somewhat smaller than those considered in the model of Ref. 36. Inclusion of further neighbor couplings (such as an antiferromagnetic third neighbor J_3) will tend to stabilize zigzag correlations [22], which is consistent with the differing ¹H and ⁷Li NMR Knight shift discussed in Ref. 33.

The specific effects of the O-H hybridization can be clearly seen by comparing the above computed interactions for the $C2/m$ structure (Fig. 1 (a)) with symmetric O-H-O bonds to those for the various lower symmetry structures (Fig. 1 (b)-(d)). We will discuss the interactions in the xyz reference frame of Fig. 2. For structure Fig. 1 (b), the doubled c -axis provides two distinct layers, with O-H distances being equal within each layer. In the H-rich layer B, the reduced $d_{OH} = 1.05$ Å results in a significant suppression of $|t_2|$, which reduces K_1 to -7 meV. In contrast, for the H-poor layer A, for which $d_{OH} = 1.49$ Å, we find an enhancement of K_1 to -23.7 meV. For structures Fig. 1 (c)-(d), the symmetry of the two Ir-O-Ir hopping paths is broken by the asymmetric hydrogen atom positions. This produces several effects. First, the lower symmetry enhances Γ'_1 , and allows for a large antisymmetric Dzyaloshinskii-Moriya interaction $\mathbf{D} \cdot (\mathbf{S}_i \times \mathbf{S}_j)$ due to breaking of local inversion symmetry. Second, the perfect balance of the hopping paths via the two bridging oxygens is disrupted, leading to an enhancement of the Heisenberg exchange J_1 , and suppression of K_1 . This trend is also followed in the presence of the H-vacancies, which we have considered in terms of structure Fig. 1 (e), which is obtained from the ideal structure Fig. 1 (a) by removing one of the H atoms for the Z-bond. This further reduces the local symmetry, leading to large J_1 , Γ'_1 and DM-interactions. Taken together, the large overall variances in the computed interactions demonstrate an extreme sensitivity to the details of the H-bonds.

Given the sensitivity of the magnetic interactions, it is crucial to determine the precise positions of the H and D atoms. Following Ref. 46 and 47, the interlayer O-H-O hydrogen bonds can be classified as strong, low-barrier,

TABLE I. Nearest-neighbor Z-bond magnetic interactions in meV for H₃LiIr₂O₆ obtained by exact diagonalization on two-site cluster for different structures employing $U = 1.7$ eV, $J_H = 0.3$ eV, $\lambda = 0.4$ eV and full crystal-field terms.

Structure	J_1	K_1	Γ_1	Γ'_1	(D_x, D_y, D_z)
(a) Ideal ($C2/m$)	-1.3	-15.4	+1.5	-5.1	(-, -, -)
(b) ($C_{2c}2/m$)					
H-Poor (Layer A)	-0.3	-23.7	-1.5	-3.3	(-, -, -)
H-Rich (Layer B)	-2.7	-7.0	+3.1	-4.0	(-, -, -)
(c) ($P2_1/m$)	-7.6	-1.6	+2.3	-9.1	(2.3, 2.3, 0.1)
(d) (Cm)	-12.0	+6.8	+2.4	-10.6	(2.7, 2.7, 0.7)
(e) H-vacancy	-16.3	+3.7	+1.6	-18.5	$\pm(6.1, 6.1, -7.2)$

or weak, depending on the shape of the energy potential as a function of hydrogen position. If the distance between the two oxygens d_{OO} is short ($\lesssim 2.4$ Å) [48], the bond is characterized either by a single-well potential or by a double-well potential with a barrier that is smaller than the vibrational zero-point energy E_0 (ZPE). In this case, the probability density $|\Psi_0^H(x)|^2$ for the H position in the vibrational ground state is expected to display a single peak at the midpoint between the O atoms. This is considered a *strong* H-bond. For larger distance ($d_{OO} \sim 2.55$ Å), the barrier typically becomes of similar magnitude to the ZPE, leading to a double peak in $|\Psi_0^H(x)|^2$. The H rapidly tunnels between the two minima, with a characteristic frequency ω^* that can be estimated from the energy difference of the lowest two vibrational levels $\hbar\omega^* \sim (E_1 - E_0)$. Provided this tunnel splitting ω^* is large compared to the experimental time scales, the dynamical fluctuations of the H will be averaged out in measurements of the magnetic response. This is termed a *low-barrier* H-bond. Finally, for still larger distances ($d_{OO} \gtrsim 2.6$ Å) the development of a large barrier suppresses tunnelling ($\omega^* \rightarrow 0$), leading to a *weak* H-bond. In this limit, the H-atoms will become increasingly localized into asymmetric O···H-O bonds on experimental time-scales.

In order to investigate the H-bond potentials for H₃LiIr₂O₆, we performed total energy calculations as a function of hydrogen positions along the O-O vector ($d_{OH} = xd_{OO}$), starting from the the experimental $C2/m$ structure of Ref. 32. There are two kinds of O-H-O bonds: bond 1 (O(1)-H-O(1)) with $d_{OO} \sim 2.46$ Å, and bond 2 (O(2)-H-O(2)) of $d_{OO} \sim 2.54$ Å. As shown in Fig. 3 (a)-(b), the potential curves for both bond types have two local minima. To estimate the ZPE, we fit the obtained potential energy curves with the form $V(x) = -Ax^2 + Bx^4$ and computed the vibrational eigenstates for the corresponding Hamiltonian $H = -\frac{\hbar^2}{2m}\nabla^2 + V(x)$. The vibrational energies $\{E_n\}$ are indicated in Fig. 3. For bond 1, the ZPE (E_0) exceeds the barrier energy, suggesting classification as a strong H-

bond. For bond 2, the ZPE lies below the barrier, leading to a double peak in $|\Psi_0^H(x)|^2$. However, the tunnel splitting remains large $\hbar\omega^* = E_1 - E_0 \sim 70$ meV compared to the magnetic interactions, suggesting classification as a low-barrier H-bond. On this basis, in pristine samples of $\text{H}_3\text{LiIr}_2\text{O}_6$, the symmetry of the O-H-O bonds should be maintained on time scales relevant to the magnetic response. The effective magnetic interactions should reflect those computed above for the ideal $C2/m$ structure Fig. 1 (a).

This conclusion, however, does not hold for $\text{D}_3\text{LiIr}_2\text{O}_6$. In similar layered structures, D-substitution tends to increase the interlayer O-O distance, e.g. on the order of 5% for (H/D) CrO_2 . [49] At the same time, the larger mass of D significantly reduces the ZPE (see Fig. 3 (d)). As a result, the propensity for deuterated systems to form asymmetric O \cdots D-O bonds is strongly enhanced [50]. For example, while the O-H-O bonds in HCrO_2 remain symmetric, DCrO_2 undergoes a structural transition at $T_c \sim 320$ K, occasioned by the formation of asymmetric bonds in the bulk [51, 52]. Similar effects [53, 54] are also observed in the deuterated organic spin-liquid candidate $\kappa\text{-D}_3\text{-(Cat-EDT-TTF)}_2$ ($T_c \sim 185$ K). We therefore computed the deuterium vibrational energies for $\text{D}_3\text{LiIr}_2\text{O}_6$ including a O-O distance of 2.54 Å (see Fig. 3 (c)), and a $\sim 5\%$ stretch of O-O distances to 2.67 Å (see Fig. 3 (d)) for bond 2. The tunnel splittings of $\hbar\omega^* \sim 30$ meV in Fig. 3 (c), and ~ 3 meV in Fig. 3 (d) suggest the formation of asymmetric O-D \cdots D bonds in $\text{D}_3\text{LiIr}_2\text{O}_6$ samples on magnetically relevant time scales. Given the similarity of the magnetic and structural energy scales, non-trivial effects of their coupling may also appear. However, the bulk magnetic interactions should differ strongly from pristine $\text{H}_3\text{LiIr}_2\text{O}_6$, reflecting those computed for e.g. structures Fig. 1 (b)-(d).

The question therefore remains whether the observed suppression of magnetic order in (H/D) $_3\text{LiIr}_2\text{O}_6$ results primarily from frustration (i.e. quantum fluctuations), or from disorder-induced inhomogeneity [37, 55, 56]. Experimentally, if both H and D systems display similar low temperature response despite differing degrees of H/D localization, it could be taken as evidence that both are dominated by disorder. Since H/D atoms near grain boundaries and crystalline defects will likely form conventional short O-H bonds, disorder effects on the interactions may be enhanced.

It is therefore relevant to consider possible sources of structural disorder. One source could be related to the H substitution through the delithiation method $\text{Li}_2\text{MO}_3 \rightarrow \text{H}_x\text{Li}_{2-2y-x}\text{MO}_{3-y}$ where the resulting compounds are generally thought to be rather disordered with variable stoichiometry (x, y) [57]. Inhomogeneity may also arise in stoichiometric samples related to the microstructure and distribution of H atoms. Due to the differing coordination environment around the O atoms, introduction of H requires the shifting of the hexagonal layers

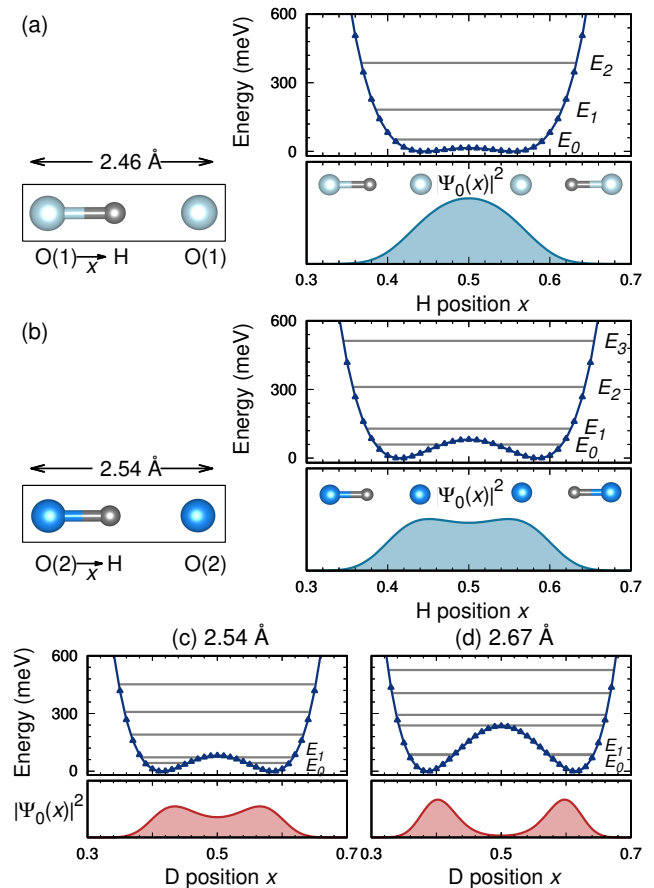


FIG. 3. Energies of the crystal with O-H distance $d_{OH} = x d_{OO}$ for (a) O(1)-H-O(1) bond 1 and (b) O(2)-H-O(2) bond 2 when fixing another hydrogen in the middle of oxygen and oxygen. (c) Energies with replacing Hydrogen by Deuterium for bond 2, and (d) replacing Hydrogen by Deuterium for bond 2 with stretching of O-O distance by 5%. $\{E_n\}$ are the vibrational energies.

with respect to each other. The resultant shear stresses have been observed to cleave the crystals along the ab -plane, producing thin platelets with numerous stacking faults [58, 59], increasing substantially the sample surface area. For isolated thin platelets, the formation of short O-H bonds at the surface would lead to strongly different interactions from the bulk. Furthermore, complete coverage of *both* the top and bottom surfaces of a platelet with H^+ would require a surplus of protons. A finite concentration of hydrogen vacancies in the sample is therefore required for charge neutrality, modifying the local interactions (i.e. structure Fig. 1 (e)). In view of the above considerations, the magnetic response is likely to be sensitive to both the stoichiometry and microstructure of the samples, through the strong influence of the H-bonds on the local interactions.

In summary, we have investigated how the introduction of hydrogen affects the structure and magnetic proper-

ties of $(\text{H/D})_3\text{LiIr}_2\text{O}_6$. The H-bond geometry strongly affects the local magnetic interactions due to hybridization with the bridging oxygen ligands. For the H-system, we conclude that the interlayer O-H-O bonds are likely to remain symmetrical in bulk pristine samples due to large zero-point fluctuations of the H positions. In this case, the estimated magnetic model lies close to the classical tricritical point between ferromagnetic, zigzag and incommensurate spiral orders. This strongly hints to a lack of magnetic order in the quantum case. Upon deuteration or in the presence of structural defects and grain boundaries, the symmetrical O-(H/D)-O bonds are destabilized, strongly modifying the local magnetic couplings. Considering previous studies, such defects may naturally arise through the method employed in the preparation of $(\text{H/D})_3\text{LiIr}_2\text{O}_6$. Given the strong sensitivity of the magnetic Hamiltonian to the H-bond geometry, further studies of the specific microstructure and composition of the samples will provide significant insight into their magnetic response.

We acknowledge useful discussions with Sananda Biswas, Vladislav Borisov, George Jackeli, Tomo Takayama and Hidenori Takagi. We acknowledge support by the Deutsche Forschungsgemeinschaft through grant SFB/TR 49 and the computer time was allotted by the Centre for Scientific Computing (CSC) in Frankfurt.

* Corresponding author: yingli@itp.uni-frankfurt.de

- [1] A. Kitaev, *Annals of Physics* **321** (2006).
- [2] G. Jackeli and G. Khaliullin, *Phys. Rev. Lett.* **102**, 017205 (2009).
- [3] S. M. Winter, A. A. Tsirlin, M. Daghofer, J. van den Brink, Y. Singh, P. Gegenwart, and R. Valentí, *Journal of Physics: Condensed Matter* **29**, 493002 (2017).
- [4] W. Witczak-Krempa, G. Chen, Y. B. Kim, and L. Balents, *Annual Review of Condensed Matter Physics* **5**, 57 (2014).
- [5] J. G. Rau, E. K.-H. Lee, and H.-Y. Kee, *Annual Review of Condensed Matter Physics* **7**, 195 (2016).
- [6] S. K. Choi, R. Coldea, A. N. Kolmogorov, T. Lancaster, I. I. Mazin, S. J. Blundell, P. G. Radaelli, Y. Singh, P. Gegenwart, K. R. Choi, S.-W. Cheong, P. J. Baker, C. Stock, and J. Taylor, *Phys. Rev. Lett.* **108**, 127204 (2012).
- [7] H. Gretarsson, J. P. Clancy, X. Liu, J. P. Hill, E. Bozin, Y. Singh, S. Manni, P. Gegenwart, J. Kim, A. H. Said, D. Casa, T. Gog, M. H. Upton, H.-S. Kim, J. Yu, V. M. Katukuri, L. Hozoi, J. van den Brink, and Y.-J. Kim, *Phys. Rev. Lett.* **110**, 076402 (2013).
- [8] F. Freund, S. C. Williams, R. D. Johnson, R. Coldea, P. Gegenwart, and A. Jesche, *Scientific Reports* **6**, 35362 (2016).
- [9] R. D. Johnson, S. C. Williams, A. A. Haghighirad, J. Singleton, V. Zapf, P. Manuel, I. I. Mazin, Y. Li, H. O. Jeschke, R. Valentí, and R. Coldea, *Phys. Rev. B* **92**, 235119 (2015).
- [10] A. Banerjee, C. A. Bridges, J.-Q. Yan, A. A. Aczel, L. Li, M. B. Stone, G. E. Granroth, M. D. Lumsden, Y. Yiu, J. Knolle, S. Bhattacharjee, D. L. Kovrizhin, R. Moessner, D. A. Tennant, D. G. Mandrus, and S. E. Nagler, *Nature Materials* **15**, 733 (2016).
- [11] A. Banerjee, J. Yan, J. Knolle, C. A. Bridges, M. B. Stone, M. D. Lumsden, D. G. Mandrus, D. A. Tennant, R. Moessner, and S. E. Nagler, *Science* **356**, 1055 (2017).
- [12] S. M. Winter, K. Riedl, P. A. Maksimov, A. L. Chernyshev, A. Honecker, and R. Valentí, *Nature Communications* **8**, 1152 (2017).
- [13] S. M. Winter, K. Riedl, D. Kaib, R. Coldea, and R. Valentí, *Phys. Rev. Lett.* **120**, 077203 (2018).
- [14] T. Takayama, A. Kato, R. Dinnebier, J. Nuss, H. Kono, L. S. I. Veiga, G. Fabbris, D. Haskel, and H. Takagi, *Phys. Rev. Lett.* **114**, 077202 (2015).
- [15] A. Biffin, R. D. Johnson, S. Choi, F. Freund, S. Manni, A. Bombardi, P. Manuel, P. Gegenwart, and R. Coldea, *Phys. Rev. B* **90**, 205116 (2014).
- [16] A. Biffin, R. D. Johnson, I. Kimchi, R. Morris, A. Bombardi, J. G. Analytis, A. Vishwanath, and R. Coldea, *Phys. Rev. Lett.* **113**, 197201 (2014).
- [17] Y. Li, S. M. Winter, H. O. Jeschke, and R. Valentí, *Phys. Rev. B* **95**, 045129 (2017).
- [18] K. A. Modic, T. E. Smidt, I. Kimchi, N. P. Breznay, A. Biffin, S. Choi, R. D. Johnson, R. Coldea, P. Watkins-Curry, and G. T. McCandless, *Nat. Commun.* **5**, 4203 (2014).
- [19] S. C. Williams, R. D. Johnson, F. Freund, S. Choi, A. Jesche, I. Kimchi, S. Manni, A. Bombardi, P. Manuel, P. Gegenwart, and R. Coldea, *Phys. Rev. B* **93**, 195158 (2016).
- [20] V. M. Katukuri, S. Nishimoto, V. Yushankhai, A. Stoyanova, H. Kandpal, S. Choi, R. Coldea, I. Rousochatzakis, L. Hozoi, and J. van den Brink, *New Journal of Physics* **16**, 013056 (2014).
- [21] J. G. Rau, E. K.-H. Lee, and H.-Y. Kee, *Phys. Rev. Lett.* **112**, 077204 (2014).
- [22] S. M. Winter, Y. Li, H. O. Jeschke, and R. Valentí, *Phys. Rev. B* **93**, 214431 (2016).
- [23] S. Ducatman, I. Rousochatzakis, and N. B. Perkins, *Physical Review B* **97**, 125125 (2018).
- [24] I. Rousochatzakis and N. B. Perkins, *Physical Review B* **97**, 174423 (2018).
- [25] I. I. Mazin, H. O. Jeschke, K. Foyevtsova, R. Valentí, and D. I. Khomskii, *Phys. Rev. Lett.* **109**, 197201 (2012).
- [26] K. Foyevtsova, H. O. Jeschke, I. I. Mazin, D. I. Khomskii, and R. Valentí, *Phys. Rev. B* **88**, 035107 (2013).
- [27] Y. Li, K. Foyevtsova, H. O. Jeschke, and R. Valentí, *Phys. Rev. B* **91**, 161101 (2015).
- [28] V. Hermann, M. Altmeyer, J. Ebad-Allah, F. Freund, A. Jesche, A. A. Tsirlin, M. Hanfland, P. Gegenwart, I. I. Mazin, D. I. Khomskii, R. Valentí, and C. A. Kuntscher, *Phys. Rev. B* **97**, 020104 (2018).
- [29] T. Biesner, S. Biswas, W. Li, Y. Saito, A. Pustogow, M. Altmeyer, A. U. B. Wolter, B. Büchner, M. Roslova, T. Doert, S. M. Winter, R. Valentí, and M. Dressel, *Phys. Rev. B* **97**, 220401 (2018).
- [30] G. Bastien, G. Garbarino, R. Yadav, F. Martinez-Casado, R. B. Rodríguez, Q. Stahl, M. Kusch, S. Limandri, R. Ray, P. Lampen-Kelley, *et al.*, *Physical Review B* **97**, 241108 (2018).
- [31] M. J. O'Malley, P. M. Woodward, and H. Verweij, *Journal of Materials Chemistry* **22**, 7782 (2012).

- [32] S. Bette, T. Takayama, K. Kitagawa, R. Takano, H. Takagi, and R. E. Dinnebier, *Dalton Trans.* **46**, 15216 (2017).
- [33] K. Kitagawa, T. Takayama, Y. Matsumoto, A. Kato, R. Takano, Y. Kishimoto, S. Bette, R. Dinnebier, G. Jackeli, and H. Takagi, *Nature* **554**, 341 (2018).
- [34] T. Takayama, APS March Meeting 2018.
- [35] J. Nasu, M. Udagawa, and Y. Motome, *Physical Review B* **92**, 115122 (2015).
- [36] K. Slagle, W. Choi, L. E. Chern, and Y. B. Kim, *Phys. Rev. B* **97**, 115159 (2018).
- [37] I. Kimchi, J. P. Sheckelton, T. M. McQueen, and P. A. Lee, arXiv:1803.00013 (2018).
- [38] J. Chaloupka, G. Jackeli, and G. Khaliullin, *Phys. Rev. Lett.* **105**, 027204 (2010).
- [39] Y. Yamaji, Y. Nomura, M. Kurita, R. Arita, and M. Imada, *Phys. Rev. Lett.* **113**, 107201 (2014).
- [40] G. Kresse and J. Furthmüller, *Comput. Mater. Sci.* **6**, 15 (1996).
- [41] J. Hafner, *J. Comput. Chem.* **29**, 2044 (2008).
- [42] P. Blaha, K. Schwarz, G. K. H. Madsen, D. Kvasnicka, and J. Luitz, WIEN2k, An Augmented Plane Wave Plus Local Orbitals Program for Calculating Crystal Properties (Karlheinz Schwarz, Techn. Universität Wien, Austria) (2001).
- [43] S. M. Winter, K. Riedl, and R. Valentí, *Phys. Rev. B* **95**, 060404 (2017).
- [44] See Supplemental Material which contains structural parameters, density of states, and hopping parameters for various structures as well as Ref 21, 26, 40–42, 60, and 61.
- [45] J. Chaloupka and G. Khaliullin, *Physical Review B* **92**, 024413 (2015).
- [46] R. H. McKenzie, C. Bekker, B. Athokpam, and S. G. Ramesh, *The Journal of chemical physics* **140**, 174508 (2014).
- [47] C. L. Perrin and J. B. Nielson, *Annual Review of Physical Chemistry* **48**, 511 (1997).
- [48] B. Schiøtt, B. B. Iversen, G. K. H. Madsen, F. K. Larsen, and T. C. Bruice, *Proceedings of the National Academy of Sciences* **95**, 12799 (1998).
- [49] A. N. Christensen, P. Hansen, and M. Lehmann, *Journal of Solid State Chemistry* **21**, 325 (1977).
- [50] T. Matsuo, A. Inaba, O. Yamamuro, and N. Onoda-Yamamuro, *Journal of Physics: Condensed Matter* **12**, 8595 (2000).
- [51] T. Matsuo, T. Maekawa, A. Inaba, O. Yamamuro, M. Ohama, M. Ichikawa, and T. Tsuchida, *Journal of molecular structure* **790**, 129 (2006).
- [52] S. Dolin, I. Flyagina, M. Tremasova, T. Y. Mikhailova, A. Gavriluk, and A. Levin, *International Journal of Quantum Chemistry* **107**, 2409 (2007).
- [53] A. Ueda, S. Yamada, T. Isono, H. Kamo, A. Nakao, R. Kumai, H. Nakao, Y. Murakami, K. Yamamoto, Y. Nishio, *et al.*, *Journal of the American Chemical Society* **136**, 12184 (2014).
- [54] K. Yamamoto, Y. Kanematsu, U. Nagashima, A. Ueda, H. Mori, and M. Tachikawa, *Physical Chemistry Chemical Physics* **18**, 29673 (2016).
- [55] I. Kimchi, A. Nahum, and T. Senthil, *Phys. Rev. X* **8**, 031028 (2018).
- [56] A. J. Willans, J. T. Chalker, and R. Moessner, *Phys. Rev. Lett.* **104**, 237203 (2010).
- [57] Y. Paik, C. P. Grey, C. S. Johnson, J.-S. Kim, and M. M. Thackeray, *Chemistry of materials* **14**, 5109 (2002).
- [58] W. Tang, H. Kanoh, X. Yang, and K. Ooi, *Chemistry of materials* **12**, 3271 (2000).
- [59] D. Weber, L. M. Schoop, D. Wurmbrand, J. Nuss, E. M. Seibel, F. F. Tafti, H. Ji, R. J. Cava, R. E. Dinnebier, and B. V. Lotsch, *Chemistry of Materials* **29**, 8338 (2017).
- [60] P. E. Blöchl, *Phys. Rev. B* **50**, 17953 (1994).
- [61] J. P. Perdew, K. Burke, and M. Ernzerhof, *Phys. Rev. Lett.* **77**, 3865 (1996).